ELSEVIER

Observations of Microcracking in Cement Paste upon Drying and Rewetting by Environmental Scanning Electron Microscopy

Knut O. Kjellsen* and Hamlin M. Jennings†
*Swedish Cement and Concrete Research Institute, Stockholm and †Department of Civil Engineering and Department of Materials and Engineering, Northwestern University, Evanston, Illinois

This study reports some preliminary observations of microcracks in hardened high performance cement paste (i.e., cement paste of low water:binder ratio). Specimens were examined at high magnifications and at relative humidities ranging from 0 to 100% in an environmental scanning electron microscope (ESEM). Direct microcracks were observed in samples that had not been dried, indicating that microcracks are probably an intrinsic feature of high performance concrete. It was further observed that the microcracks widened upon drying and closed again upon rewetting. Some practical consequences of these findings are discussed briefly. ADVANCED CEMENT BASED MATERIALS 1996, 3, 14–19

KEY WORDS: Drying, Electron microscopy, Environmental scanning, High performance concrete, Microcracking, Rewetting, Self-desiccation

The question of microcracks in cementitious materials, and in particular the development of cracks under mechanical stress, has been investigated and reported in the literature [1–5]. Research has also focused on the development of cracks as a result of stress due to drying [6,7]. However, some confusion exists due to inconsistent results. For instance, some researchers [4,5] report the presence of a fracture process zone ahead of a continuous propagating macrocrack, whereas others [8,9] do not find evidence of such a zone of discontinuous microcracks. Confusion originates, at least in part, from the lack of a good definition of microcracks and from how microcracks would be observed using various experimental techniques. The term "microcrack" is frequently used, rather uncritically, although some definitions have been suggested. Slate and Hover [10] defined microcracks as cracks having a width of less than 100 μm, while still being detectable. Jensen [11] defines microcracks as extended faults with a width of less than 10 μm, which facilitate fast transport of fluids or gases through the concrete. The different definitions appear to be closely related to the experimental technique used and to the orientation of the studies.

For this study, we propose a definition of microcracks based on previous definitions that we consider to be reasonable, physical interpretations of microcracks. The upper limit for microcracks will be set at 10 μm. The lower limit will be defined as a separation resulting from overstepping the local strain capacity, such that there is no stress transferred across the "crack." This definition implies that the lower limit presumably will be on the nanometer scale and, thus, probably not detected by scanning electron microscopy or any of the other commonly applied methods for studying microcracks. As a consequence, there might be microcracks in the specimens under study that are not detected. One should be aware of this possibility in any study of microcracks.

The various techniques used to study microcracks can be divided into indirect or direct methods. Examples of indirect methods are measurements of compliance, ultrasonic pulse velocity, acoustic emission, mercury penetration, and numerical simulations. A common characteristic of indirect methods is that the presence of microcracks, or the extent of microcracking, is deduced from information that is only indirectly related to microcracks. These methods generally cannot give any detailed information about microcracking. The direct methods are techniques of direct physical observation, such as

Address correspondence to: Hamlin M. Jennings, Department of Civil Engineering, Northwestern University, 2145 Sheridan Road, Room A 133, Evanston, Illinois 60201.
Received June 24, 1994; Accepted April 19, 1995

ISSN 1065-7355/96/$15.00
SSDI 1065-7355(95)00030-U

optical microscopy and scanning electron microscopy. Chatterji et al. [12] and Hwang and Young [7] have studied the effect of drying shrinkage on crack formation using optical microscopy. Hwang and Young [7] have also studied the effect of specimen thickness on shrinkage and cracking using light microscopy. They prepared thin cement paste specimens that were probably wet-cured. Using both dark-field and bright-field illumination techniques, they reported that microcracking occurred at the beginning of drying whenever the thin specimen (thickness less than 2 mm) was suddenly exposed to low relative humidity (RH; 50%) but that the cracks eventually closed up. Therefore, they do not contribute to values of shrinkage at equilibrium.

Chatterji et al. [12] observed some cracking after drying. They cast discs of cement paste of 25 mm diameter/1.5 mm thickness that were moist-cured for 6 weeks before being dried over silica gel. Using a fluorescent dye to highlight the cracks, they observed some microcracking only in the thin section. They reported that the fluorescent epoxy had penetrated into the disc along the preexisting cracks and then had spread to both sides of the cracks, making the cracks highly visible.

Optical microscopy has a limited resolution compared to scanning electron microscopy. Scanning electron microscopy has been used to study the process of cracking due to mechanically induced stress [4,5,13,14]. Mindess and Diamond [13] studied the crack propagation in mortars with a device for mechanically loading a sample in the SEM specimen chamber. In this way, the crack propagation could be studied. They reported that several fine cracks existed before mechanical loading, and they hypothesized that these fine cracks were due to drying shrinkage. It was clear, according to the authors, that these fine cracks were not continuous, and they did not appear to extend very far into the specimen. During loading, crack branching appeared. These were fairly widely spaced and did not appear to form a continuous network at the magnification used. Inactive branch cracks were not widened by further extension of the main crack. Although some attempts have been made [14,15] to prevent drying in an SEM, the highest pressure achieved was between 0.5 and 1 torr, which, at room temperature, corresponds to a relative humidity between 10 and 20% and, thus, will cause drying. Diamond et al. [15] claimed that with their system, extensive drying was prevented because air saturated with water vapor, was drawn into the specimen chamber.

The vacuum in the specimen chamber of the SEM is a major drawback when studying cracks in cementitious materials. Ollivier [16] developed a technique where a replica of the specimen, instead of the specimen itself, is studied by scanning electron microscopy. A thin film of bioden is applied to the specimen's surface to provide an imprint of the surface structure. The replica, which is dimensionally stable on drying, is studied in the SEM. The advantage of the replica technique is that the cementitious specimen is not exposed to the vacuum; however, the rather tedious preparation of the surface of the cementitious specimen may influence the imprint. The resolution was claimed to be better than 0.5 μm. Opara [5] hypothesized that the viscosity of the material used for producing the replica could be a limiting factor because small cracks will not be intruded effectively. Under direct SEM or optical microscopic examination, a zone of microcracks was observed. Massat et al. [17] studied microcracking of high performance concrete cured under moisture-sealed conditions and reported that microcracks existed in the external, undried state. Bascoul et al. [9,18] and Ringot [19] studied mechanically induced cracks by the replica technique, whereas Bascoul et al. [20] made a comparative study by stereophotography, speckle laser, and the replica technique with no definitive conclusions. Diamond et al. [15] studied cracking in mortars under load using the backscattered electron mode of a SEM equipped with a "wet cell." As far as the present authors are aware, this is the only previous attempt for studying cracking at relatively high pressures in the SEM.

This paper reports results of experiments where the relative humidity is controlled, as opposed to experiments where the specimen is subjected to the vacuum of an SEM. In other words, cracks due to drying, not mechanical stress, are investigated. The present work concentrates on the experimental techniques. Preliminary observations are reported of microcracks in hardened high performance cement paste (i.e., low water: binder ratio cement paste) using environmental scanning electron microscopy. The paper is part of a larger project using environmental scanning electron microscopy for studying microcracks in mature cement paste, the results of which will be presented at a later stage.

Drying of cement-based materials causes shrinkage and, thus, some rearrangement of the solid matter. This may lead to microcracking. The ESEM maintains most of the advantages associated with the conventional SEM such as high spatial resolution and large depth-of-focus, but observations of materials in a moist environment are possible. In addition, coating of the sample with a conductive material to prevent charging is not needed with the ESEM.

Specimens may be observed at 20 torr of water pressure, implying that 100% RH can be obtained at 22°C. The image clarity, however, is poor at this pressure, but it improves considerably at somewhat lower pressures. A Peltier cooling stage allows small specimens to be cooled so that a high relative humidity can be maintained close to the specimen at a relatively low speci-

Adv Cem Bas Mat
1996;3:14–19

men chamber pressure, while still providing very good image clarity (e.g., 100% RH occurs at 9.2 torr at 10°C instead of 20 torr at 22°C). Thus, liquids can be studied and water can be condensed on a specimen surface. Indeed, the specimen temperature and the pressure can be regulated so that relative humidities ranging from 100 to almost 0% are maintained. This makes it possible to study the dynamic effect of drying and wetting. Studying water-saturated materials is somewhat problematic because the electrons are absorbed into liquid water and, thus, the solid is not observed [21]. On low atomic number materials, high-angle relief contrast is much greater than on high atomic number materials. Thus, the brightness at steep angles of water drops or similar objects are very bright and flat areas are very dark [22]. A review describing the principles and functions of the ESEM in more detail is given elsewhere [23,24].

Experimental

Method

The microscope was operated in the environmental secondary detector (ESD) mode and the accelerating voltage was held at 20 kV. Prior to the experiment, the specimen was cooled to 10°C in a refrigerator, and it was maintained at 10°C during the ESEM examination. The specimen chamber pressure was generally maintained between 8.3 and 3.9 torr, corresponding to relative humidities between 90 and 40%.

Two control experiments were carried out to ensure that the main experiment is not misinterpreted. First, a test of resolution was performed in the ESD mode. Small alumina particles, nonreactive to water, were studied at pressures and relative humidities similar to those used for the cement paste specimens in the main study. The result is given in Figure 1a and b. The particles were exposed to 100% RH before Figure 1a was obtained, and, as can be seen from the lower left particle, some liquid water still remains at the time of image collection. However, a comparison of the two other particles in the two micrographs reveals no apparent difference in resolution. Thus, possible artifacts due to pressure-dependent resolution should be excluded.

The second control experiment was used to investigate the effect of lowering the specimen temperature from 20°C (curing temperature) to 10°C (experimental temperature). A specimen was studied first at 20°C and 7.0 torr and then, 15 minutes later, at 10°C and 3.7 torr. Both sets of conditions maintain a relative humidity of 40%. The results are depicted in Figure 2a and b in which the width of the microcracks is apparently similar. Thus, the thermal contraction, due to the 10°C temperature decrease, is presumably too small to have any significant influence on the development of the microcracks reported in this paper.

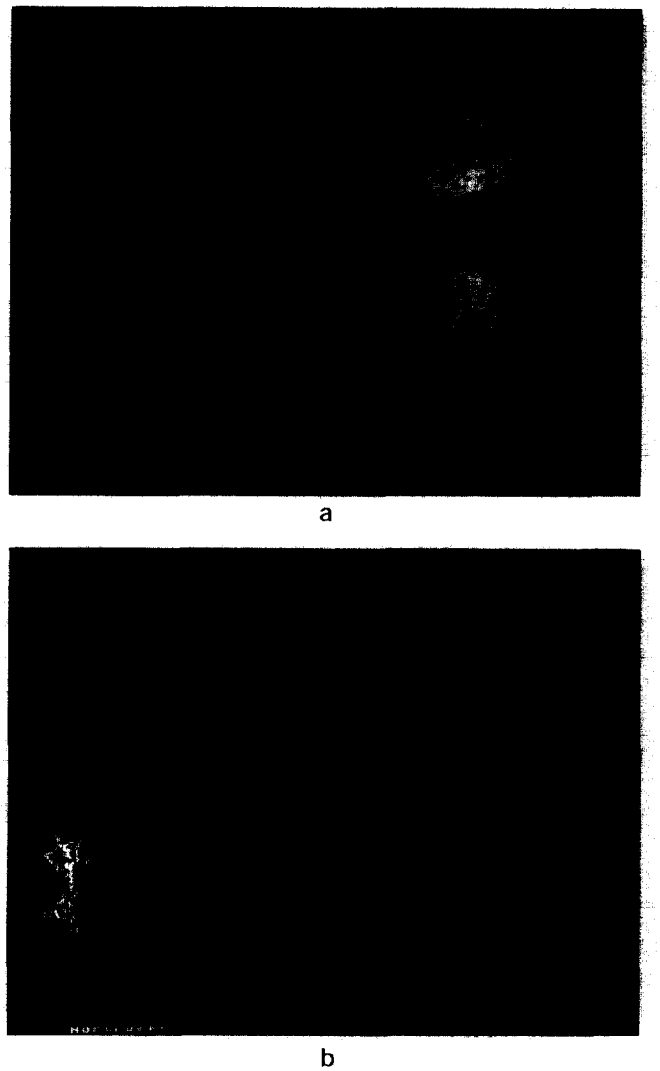

FIGURE 1. Alumina particles observed in the ESEM. (a) 80% RH; (b) 20% RH.

Materials and Specimens

Cement paste specimens were made of portland cement, silica fume, deionized water, and a superplasticizer. The cement was a Swedish sulfate-resistant cement. The silica fume was in slurry form and contained 50% silica. The characteristics of the cement and silica are given in Table 1. The plasticizer was added as a solution of 40% sulphonated naphthalene formaldehyde, 0.3% tribetyl phosphate, and water. One mix was made. The water:binder (w:b) ratio was held at 0.25, and the binder fraction was composed of 90% cement and 10% silica fume, by weight. The amount of plasticizer was 4% of the binder weight. The ingredients were thoroughly mixed, first in a Hobart mixer and then by

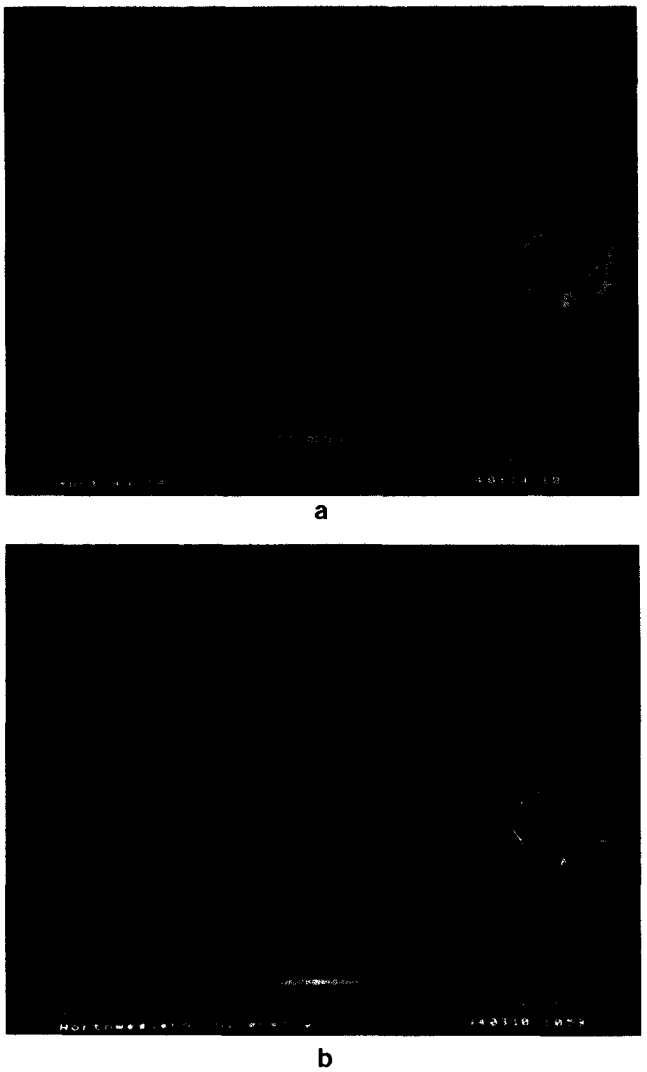

FIGURE 2. Cement paste specimen. (a) 20°C and 40% RH; (b) 10°C and 40% RH.

a high-speed dispersion tool. The detailed mixing procedure ensured a very smooth paste with presumably very few silica agglomerates.

The mix was cast into forms that consisted of two sections separated by a flat and smooth plate made of Plexiglas. On the first block, small (8-mm diameter) rubber O-rings were fastened to a plate. The fresh paste was poured into the compartments (within the O-ring) and gently vibrated. The second block was then placed on top and the sandwich of O-rings between the blocks was carefully pressed and screwed together. The forms were then rotated for 1 day, to prevent segregation of the paste, before the forms were opened. The specimens were then placed in small tight glass bottles containing only a very small amount of air. This ensured sealed curing conditions with practically no moisture exchange or carbonation. All mixing and curing took place at 20°C. The specimens had a diameter of approximately 8 mm and a height of about 1 mm and were cured for approximately 8 months before being examined in the ESEM. During the ESEM examination, the specimen was attached to the Peltier cooling stage by rubber cement. The flat surfaces (unpolished) of the samples were examined. After the specimens were mounted, the specimen chamber was pumped down to approximately 8.3 torr, while the specimen was maintained at 10°C, providing a relative humidity of approximately 90%.

TABLE 1. Characteristics of the cement and silica fume

Characteristics	Cement	Silica Fume
SiO_2	22.2%	94.2%
CaO	64.9%	0.26%
Al_2O_3	3.4%	0.95%
Fe_2O_3	4.8%	0.62%
MgO	0.91%	0.65%
SO_3	2.0%	0.33%
K_2O	0.56%	—
Na_2O	0.04%	0.30%
Loss on ignition	0.63%	1.79%
Fineness	302 m^2/kg	23.0 m^2/g
Specific weight	3220 kg/m^3	1798 kg/m^3
C_2S (Bogue)	19.8%	—
C_3S	58.1%	—
C_3A	0.82%	—
C_4AF	14.5%	—

Results and Discussion

Figure 3a shows an image of paste at 90% RH. A crystal grain, probably CH, can be seen at the top of a horizontal crack system just below the middle and a vertical crack to the right of the crystal. The vertical crack appears to have a maximum width of approximately 100 nm, and the horizontal crack is a few times wider. Because the paste has not yet been dried, these cracks are probably a result of internal drying, known as self-desiccation. In particular, the low initial water content may cause considerable self-desiccation, which may lead to autogenous shrinkage and microcracking as hypothesized by Chatterji [25].

Figure 3b shows the same region as in Figure 3a, after the pressure has been reduced to 3.9 torr, corresponding to 40% RH. At the time the image was obtained, the specimen had been exposed to this humidity for 15 minutes. The crack system has developed in the sense that the crack width has increased by several times. After the drying sequence, the pressure was returned to 8.3 torr (90% RH). Figure 3c shows the same area 5 minutes after the pressure was increased. The cracks have largely closed. To study the effect of swelling in somewhat more detail, the pressure was again lowered to 40% RH. Figure 4a shows another crack system at a

Advn Cem Bas Mat
1996;3:14–19

a

b

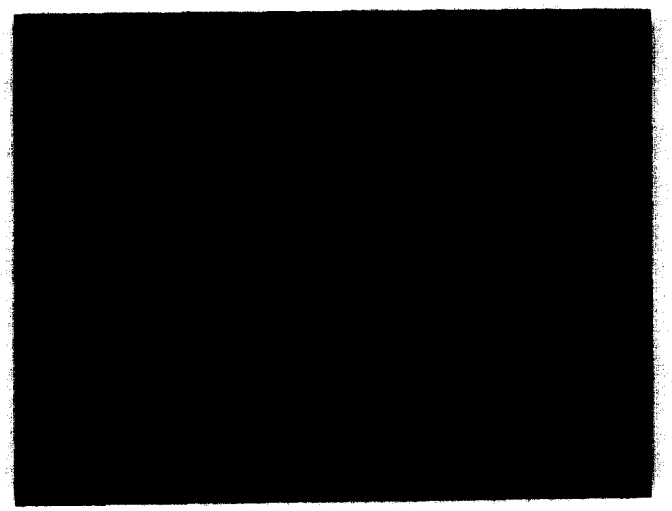

c

FIGURE 3. Cement paste specimen (a) before drying (90% RH); (b) after drying at 40% RH; and (c) after rewetting at 90% RH.

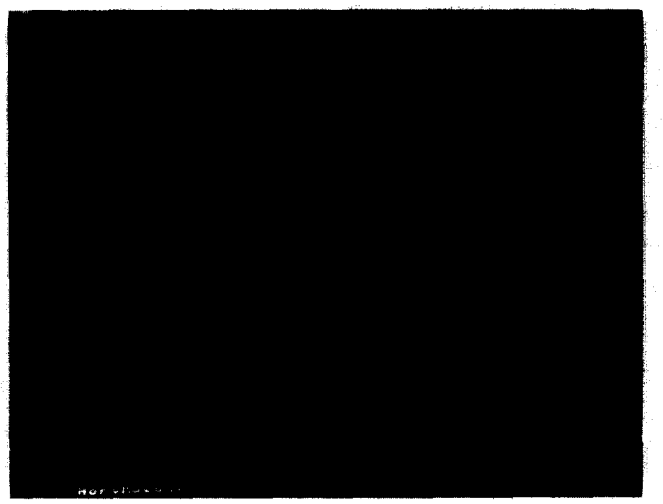

a

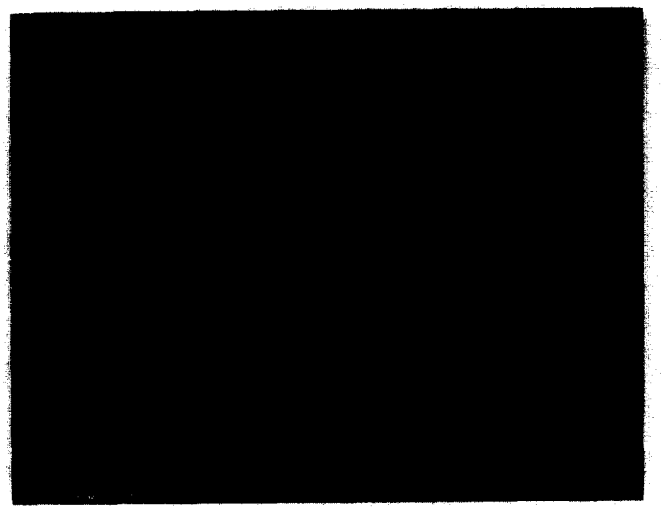

b

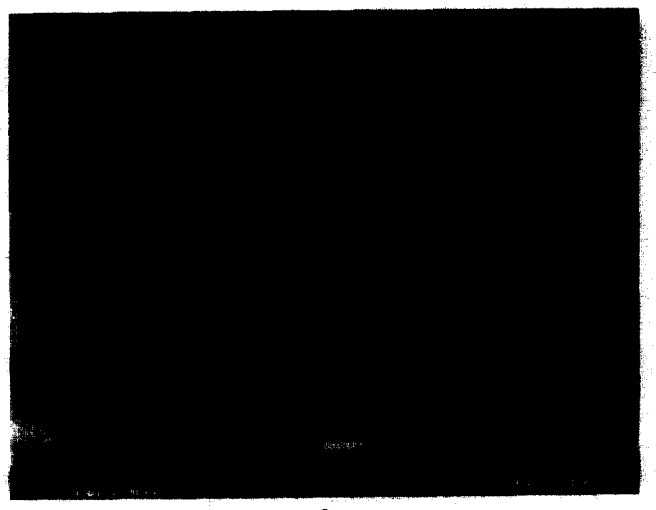

c

FIGURE 4. Cement paste specimen (a) after drying at 40% RH; (b) after rewetting at 60% RH; and (c) after rewetting at 80% RH.

higher magnification than those in Figure 3. As can be seen, the crack width is about 500 nm after drying. The pressure was raised in two steps, corresponding to relative humidities of approximately 60 and 80%. Figure 4b shows the crack system after 5 minutes at 60% relative humidity, and Figure 4c shows the crack system after another 5 minutes at 80%. It is evident that the crack width narrows as the humidity increases. Occasionally the image on the screen was held live during the drying or wetting process, and it was observed that most of the changes occurred during the first minute or so after the pressure was changed. Reducing the relative humidity to nearly 0% did not, apparently, increase the crack width compared to that at 40% RH. The analysis, however, was based on observations of the images purely by the naked eye, and small differences could not be detected. Furthermore, any equilibrium state between the specimen and the surrounding environment is not expected, due to the short drying and wetting periods.

This research may have important practical implications. Because cracks close when the material is rewetted, permeability to water in the interior of high performance concrete may not be as serious a problem as is suggested by the observation that cracks form due to self-desiccation. However, permeability to other materials such as alcohols and oils may be significant.

Conclusions

1. Environmental scanning electron microscopy is a versatile tool for studying cement paste. Undisturbed specimens can be studied at fairly high magnifications and at relative humidities ranging from 100 to almost 0%.
2. The results reported here show direct evidence of microcracks in mature high performance cement paste. Microcracks were observed initially in the externally undried state (approximately 90% RH). This observation indicates that microcracks might be an intrinsic feature of high performance concrete.
3. Upon drying, the microcracks widened as a result of shrinkage.
4. Upon rewetting, the microcracks closed again giving some indication of swelling.

Acknowledgments

We gratefully acknowledge the financial support provided by the Swedish research consortium of high performance concrete structures. The group consist of Cementa, Elkem Materials, Euroc Beton, NCC Bygg, Skanska, Strängbetong, and the government authorities BFR and Nutek. We would also like to thank Marina Reider who assisted in the microscopy. Support of the environmental scanning electron microscopy is provided through grants from Department of Energy (award No. DE-FG02-91ER45460) and the NSF Science and Technology Center for Advanced Cement-Based Materials (award No. DMR 9120002).

References

1. Richart, F.E.; Brandtzaeg, A.; Brown, L. *A Study on the Failure of Concrete Under Combined Compressive Stresses;* Bulletin No. 185; University of Illinois Engineering Experiment Station: Urbana, 1929; p. 102.
2. Hsu, T.T.C.; Slate, F.O.; Sturman, G.M.; Winter, G. *ACI J* **1963,** *60,* 209–224.
3. Shah, S.P.; Chandra, S. *ACI J.* **1965;** *65,* 770–781.
4. Tait, R.B.; Garrett, G.G. *Cem. Concr. Res.* **1986,** *16,* 143–155.
5. Opara, N.K. *ACI Mater. J.* **1993,** *90,* 618–626.
6. Bazant, Z.P.; Raftshol, W.J. *Cem. Concr. Res.* **1982,** *12,* 209–226.
7. Hwang, C.-L.; Young, J.F. *Cem. Concr. Res.* **1984,** *14,* 585–594.
8. Schlangen, E.; van Mier, J.G.M. *Cem. Concr. Comp.* **1992,** *14,* 105–118.
9. Bascoul, A.; Detriche, C.H.; Ollivier, J.P.; Turatsinze, A. In *Fracture of Concrete and Rock; Recent Developments;* Shah, S.P.; Swartz, S.E.; Barr, B., Eds.; Elsevier Applied Science: New York, 1989; pp. 327–336.
10. Slate, F.O.; Hover, K.C. In *Fracture Mechanics of Concrete: Material Characterization and Testing;* Carpinteri, A.; Ingraffea, A.R., Eds.; Martinius Nijhoff Publishers: Dordrecht, The Netherlands, 1984; pp. 137–159.
11. Jensen, A.D. Submitted for publication.
12. Chatterji, S.; Thaulow, N.; Cristensen, P. *Cem. Concr. Res.* **1981,** *11,* 155–157.
13. Mindess, S.; Diamond, S. *Cem. Concr. Res.* **1980,** *10,* 509–519.
14. Mindess, S.; Diamond, S. *Cem. Concr. Res.* **1982,** *12,* 569–576.
15. Diamond, S.; Mindess, S.; Lovell, J. *Cem. Conc. Res.* **1983,** *13,* 107–113.
16. Ollivier, J.P. *Cem. Concr. Res.* **1985,** *15,* 1055–1060.
17. Massat, M.; Ollivier, J.P.; Yssorche, M.P. In *Proceedings of the Fourth EuroSeminar on Microscopy Applied to Building Materials;* Visby, Sweden, 1993; p. 13.
18. Bascoul, A.; Ollivier, J.P.; Poushanchi, M. *Cem. Concr. Res.* **1989,** *19,* 81–88.
19. Ringot, E. *Cem. Concr. Res.* **1988,** *18,* 933–942.
20. Bascoul, A.; Benaija, E.H.; Berthaud, Y.; Torrenti, J.M.; Zizi, Z. *Cem. Concr. Res.* **1993,** *23,* 1340–1350.
21. Sujata, K.; Jennings, H.M. *J. Am. Ceramic Soc.* **1992,** *75,* 1669–1673.
22. Peter, K-R. *Environmental Scanning Electron Microscopy: SEM High Gas Pressures.* Lehigh: Advanced Imaging, 1989; p. 15.
23. Danilatos, G. D. *Scanning* **1990,** *12,* 23–27.
24. Sujata, K.; Jennings, H. M. *Advances in Scanning Electron Microscopy.* Material Research Society, March, 1991; 41–45.
25. Chatterji, S. *Cem. Concr. Res.* **1982,** *12,* 371–376.